GAS TRANSPORT PROPERTIES OF POLYBENZIMIDAZOLES WITH BULKY SUBSTITUENTS

Cite this: *INEOS OPEN*, **2024**, *7 (6)*, 185–188
DOI: 10.32931/io2457a

Received 29 October 2024,
Accepted 10 January 2025

http://ineosopen.org

A. Yu. Alentiev,[a] R. Yu. Nikiforov,*[a] V. E. Ryzhikh,[a] Yu. A. Volkova,[b] and I. I. Ponomarev[b]

[a] *Topchiev Institute of Petrochemical Synthesis, Russian Academy of Sciences, Leninskii pr. 29, Moscow, 119991 Russia*
[b] *Nesmeyanov Institute of Organoelement Compounds, Russian Academy of Sciences, ul. Vavilova 28, str. 1, Moscow, 119334 Russia*

Abstract

This work deals with the gas transport characteristics at 35 °C of two new polybenzimidazoles (PBIs) previously synthesized at INEOS RAS for use in high-temperature fuel cells: PBIs with bulky phosphonethylated substituents (PBI-O-PhT-P) and PBIs with bulky substituents and a hexafluoroisopropylidene group in the main chain (PBI-4MeO-6F). It is shown that both of these polymers are moderately permeable polymers and, in terms of hydrogen permeability, are at the level of previously studied PBIs with bulky or fluorinated substituents. PBI-O-PhT-P exhibits irregular transport parameters for CO_2, indicating specific interactions of CO_2 with the polymer. Despite the low selectivity values, taking into account an increase in the selectivity of H_2/CO_2 with temperature, there is every reason to assume that the studied PBIs are promising for the processes of high-temperature hydrogen separation.

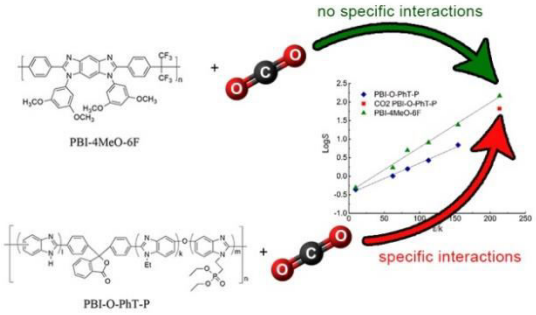

Key words: polybenzimidazoles, gas transport parameters, high temperature hydrogen recovery.

Introduction

In recent years, the investigations on gas separation properties of polybenzimidazoles (PBIs) have received increased interest. This is not only due to the successful use of these materials as membranes in high-temperature fuel cells [1], but also due to their application in high-temperature processes of hydrogen recovery and purification [2]. For example, by far the most common industrial methods of producing hydrogen are coal gasification or steam conversion of methane followed by the water–gas shift reaction at 190–350 °C. The resulting hydrogen-containing gas mixture contains about 20% of CO_2, as well as methane, water vapor and some CO and, in the case of coal gasification, hydrogen sulfide. It would be energetically advantageous to separate hydrogen from this mixture at its operating temperature using membrane gas separation [3]. To solve this problem, it is necessary to develop new membranes based on highly selective film-forming polymers operating at high temperatures (>250 °C) in an aggressive medium with no time limits, which would significantly increase the economic performance of hydrogen recovery processes. Among the polymers with such extreme characteristics, PBIs are considered as the most promising ones [2, 4–8]. Most PBIs have barrier characteristics at room temperatures; however, with increasing temperature, the permeability of hydrogen and the selectivity of the target H_2/CO_2 gas pair increase sharply [2]. For example, the commercial PBI Celasol (PBI Performance Products, Inc. (Charlotte, NC)) [2, 4–8], the so-called m-PBI (Fig. 1), which is also widely used for the production of high-temperature fuel cell membranes, is considered as a promising material for high-temperature hydrogen recovery [1]. The industrial synthesis of this polymer is carried out by solid-phase polycondensation of diphenyl isophthalate and 3,3',4,4'-tetraaminodiphenyl ether. The gas transport parameters of m-PBI at temperatures close to room temperature differ significantly in various studies (see Table 1), apparently, because of the different procedures of film preparation.

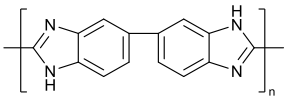

Figure 1. Chemical structure of m-PBI.

Pesiri *et al.* [9] showed that, when the temperature rises to 250 °C, the value of $P(H_2)$ for m-PBI increases to 16 Barrers, while the value of $\alpha(H_2/CO_2)$ remains the same. Li *et al.* [14] reported that $P(H_2)$ increases to 77 Barrers and $\alpha(H_2/CO_2)$ increases to 23. This combination of transport parameters makes

Table 1. Experimental transport parameters for m-PBI obtained at temperatures close to room temperature

T, °C	$P(H_2)$, Barrer[a]	$\alpha(H_2/CO_2)$	$\alpha(H_2/CH_4)$	$\alpha(H_2/N_2)$	Ref.
25	0.09	9	–	–	[9]
35	0.6	3.8	350	130	[10]
35	1.1	11	–	–	[11]
35	2	12	–	–	[12]
35	2.4	24	4600	300	[13]
43	4.0	17	–	360	[14]

[a] 1 Barrer = 10^{-10}·cm^3·(STP)·cm/(cm^2·s·cmHg).

it possible to consider it as a promising material for high-temperature hydrogen recovery.

In addition to m-PBIs, PBIs of other chemical structures have been actively studied in recent years (Fig. 2) in order to increase the gas permeability at temperatures close to room temperature.

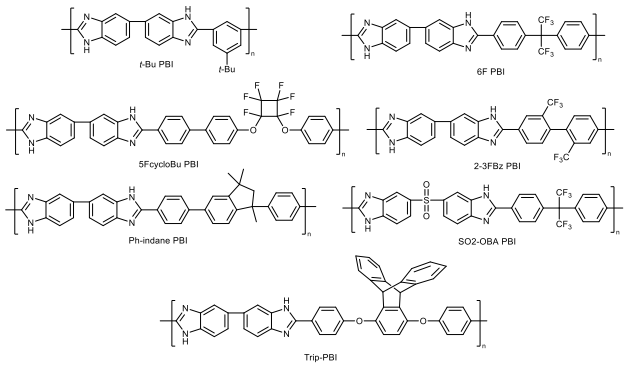

Figure 2. Chemical structures of the PBIs explored in recent years.

As can be seen from Fig. 2, the main elements of the chemical design of PBIs with increased gas permeability are the introduction of bulky and fluorinated groups, loosening the packing of polymers into derivatives of aromatic diacids, or the modification of a tetraamine moiety. The gas transport parameters of PBIs of various chemical structures at temperatures close to room temperature are presented in Table 2.

Table 2. Experimental data on the gas transport and gas separation properties for PBIs of various chemical structures

PBI	*T*, °C	$P(H_2)$	$\alpha(H_2/CO_2)$	$\alpha(H_2/CH_4)$	$\alpha(H_2/N_2)$	Ref.
t-Bu	35	10.7	5.6	210	180	[10]
6F	35	12.9	4.4	170	92	[10]
6F	44	273	1.6	–	29	[14]
5FcycloBu	34	37	2.3	–	52	[14]
2-3FBz	33	120	2.4	–	35	[14]
Ph-indane	35	37	2.0	–	50	[14]
SO_2-OBA	35	5.4	6.2	890	300	[13]
SO_2-*m*-Ph	35	3.2	19	2500	1000	[13]
SO_2-*p*-Ph	35	3.7	13	2200	690	[13]
Trip	50	116	3.5	–	–	[15]

As can be seen from Table 2, the most effective way to increase the gas permeability of PBIs is the introduction of bulky and fluorinated groups into the repeating unit of PBIs. The values of $P(H_2)$ and $\alpha(H_2/CO_2)$ sharply increase with a temperature rise for all these polymers [2, 13–15].

Recently, new PBIs for high-temperature fuel cells featuring the aforementioned properties were synthesized at INEOS RAS: phosphonethylated PBI-O-PHT (PBI-O-PhT-P) with bulky substituents [16] and fluorinated PBI-4MeO-6F [17], also containing bulky substituents (see Fig. 3). Due to their novelty, the purpose of this work was to study the gas transport properties of these PBIs.

Results and discussion

Table 3 shows the densities, free volume, permeability coefficients, and ideal selectivity for some gas pairs for the PBIs under consideration.

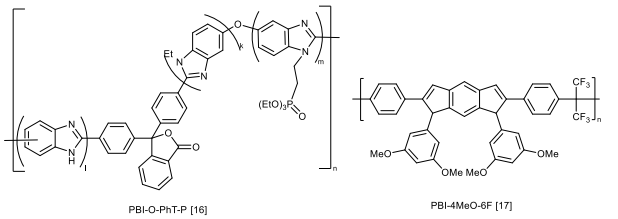

Figure 3. Chemical structures of the PBIs explored in this work.

Table 3. Permeability coefficients, density, free volume, and ideal selectivity for some gas pairs for the PBIs under consideration

Polymer	PBI-O-PhT-P	PBI-4MeO-6F	Polymer	PBI-O-PhT-P	PBI-4MeO-6F
Gas	*P*, Barrer		Gas pairs	α	
He	9.06	36	O_2/N_2	4.0	3.6
H_2	9.66 [17]	41.1 [17]	CO_2/CH_4	22	27
O_2	0.88 [17]	7.15 [17]	CO_2/N_2	24	27
N_2	0.22 [17]	1.97 [17]	H_2/CO_2	1.8	0.8
CO_2	5.38	53	H_2/N_2	44	21
CH_4	0.25	1.95	H_2/CH_4	39	21
ρ, g/cm^3	1.277	1.342	He/N_2	41	18
FFV, %	11.3	11.8	He/CH_4	36	18

The data in Table 3 obtained at 35 °C indicate low permeability and selectivity of both PBI-O-PhT-P and PBI-4MeO-6F. The free volume in these polymers is in the range of 11–12%, as for most industrial polymers. At the same time, according to the level of permeability coefficients, PBI-4MeO-6F belongs to the so-called moderately permeable, conventional polymers [18], while PBI–O-PhT-P is at the upper boundary of a low-permeable group of polymers. In terms of $P(H_2)$, both polymers exceed m-PBI (Table 1) and SO_2-containing PBIs (Table 2). At the same time, PBI-O-PhT-P appears to be close to *t*-Bu PBI (Table 2) with a bulky substituent, and PBI-4MeO-6F is close to Ph-indane PBI with a bulky substituent and to fluorinated 5FcycloBu PBI (Table 2). Nevertheless, in terms of selectivity for all gas pairs, both PBI-O-PhT-P and PBI-4MeO-6F are significantly inferior to moderately and low-permeable PBIs (Tables 1 and 2).

Table 4 shows the experimental diffusion coefficients and solubility coefficients calculated by the corresponding equation (see the Experimental section) for the PBIs explored.

The diffusion coefficients for both polymers significantly exceed the data obtained for other PBIs [10, 13]. Thus, $D(CO_2)$ comprises approximately $2\cdot10^{-10}$ cm^2/s [13] and $8\cdot10^{-10}$ cm^2/s

Table 4. Diffusion and solubility coefficients for the PBIs explored

Polymer	PBI-O-PhT-P	PBI-4MeO-6F	PBI-O-PhT-P	PBI-4MeO-6F
Gas	$D\cdot10^8$, cm^2/s		$S\cdot10^3$, cm^3(STP)/(cm$^3\cdot$cmHg)	
He	210	730	0.4	0.5
H_2	95	240	1.0	1.7
O_2	3.3	8.8	2.7	8.1
N_2	1.4	3.2	1.6	6.2
CO_2	0.81	3.6	66	150
CH_4	0.36	0.8	6.9	24

[10] for SO_2-p-Ph-PBI and m-PBI, respectively, which is at least an order of magnitude less than $D(CO_2)$ for PBI-O-PhT-P (Table 4). *t*-Bu PBI features permeability comparable to that of PBI-O-PhT-P, while $D(CO_2)$ is approximately $1.5 \cdot 10^{-8}$ cm^2/s [10], which is slightly higher than that of PBI-O-PhT-P (Table 4), but significantly lower than that of PBI-4MeO-6F (Table 4). $D(H_2)$ is about $1 \cdot 10^{-8}$ cm^2/s [10] for m-PBI and about $30 \cdot 10^{-8}$ cm^2/s [10] for *t*-Bu PBI, which is less than that for both PBI-O-PhT-P and PBI-4MeO-6F (Table 4).

Based on the traditional correlation approach [19, 20], the gas diffusion coefficients should be related by a linear correlation with the square of the effective kinetic diameter *d* and the parameters K_1 and K_2 specific for each polymer:

$$\log D = K_1 - K_2 d^2, \quad (1)$$

and the gas solubility coefficients should be related with the effective Lennard-Jones potential for the gas–gas interaction ε/k and the parameters K_3 and K_4 specific for each polymer:

$$\log S = K_3 + K_4 \frac{\varepsilon}{k}. \quad (2)$$

Based on Equations 1 and 2 and the data presented in Table 4, the dependences were constructed for both polymers (Fig. 4).

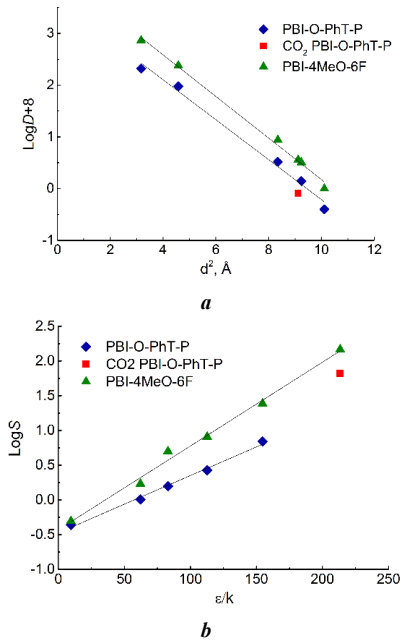

Figure 4. Dependences of the diffusion coefficients (***a***) on the effective kinetic diameter of gas molecules and the solubility coefficients (***b***) on the effective Lennard-Jones potentials for PBI-O-PhT-P and PBI-4MeO-6F.

For PBI-O-PhT-P, the linearization of the dependences was carried out excluding data for CO_2, since for the dependence according to equation (2), the points for CO_2 deviate significantly from a straight line (Fig. 4b), as for some polymers with pronounced specific interactions with CO_2 [21, 22]. With such specific interactions, the CO_2 diffusion coefficient becomes lower than in the absence of a specific interaction (Fig. 4a), while the solubility coefficient is significantly higher (Fig. 4b), which indirectly indicates the existence of specific interactions [21, 23]. Therefore, for PBI-O-PhT-P, CO_2 was presumably considered as an "interacting" gas, and the others were considered as "non-interacting" gases [21]. No deviations were observed for PBI-4MeO-6F; therefore, the data for CO_2 were included in the general dependence. The determination coefficients R^2 of all linear dependences presented in Fig. 4 exceed 0.99.

It is possible that the presence of an ethyl phosphonate group in PBI-O-PhT-P leads to the formation of centers of specific interaction with CO_2 in the polymer. Nevertheless, it is known that the solubility of CO_2 in such polymers will decrease sharply with increasing temperature, which should lead to a significant increase in the H_2/CO_2 selectivity. Nevertheless, the prospects for using PBI-O-PhT-P as a membrane material for high-temperature gas separation are low, since it was shown that this polymer is stable only up to 200 °C during prolonged heating, although the TGA analysis for the polymer upon heating at a rate of 10 °C/min showed that the temperature of the beginning of polymer decomposition is 360 °C [16]. The prospects of using PBI-4MeO-6F for high-temperature gas separation are also low, since at room temperature the selectivity of H_2/CO_2 is less than 1. However, with increasing temperature, the selectivity of H_2/CO_2, as a rule, increases due to a sharp decrease in the solubility of CO_2 [4] and low values of the activation energy of permeability [24]. Therefore, in future studies, the experimental data for both polymers must be obtained at elevated temperatures.

Experimental section

PBI-O-PhT-P films with a thickness of ~30 microns were cast from a solution in NMP on glass substrates or on a MEMCAST installation with subsequent drying at 150 °C. PBI-4MeO-6F films were obtained from 5% reaction solutions of prepolymers (polyamides) in DMAA on glass substrates or on a MEMCAST installation followed by thermal cyclization under vacuum at 300 °C [17].

The permeability and diffusion coefficients of H_2, He, N_2, O_2, CO_2, and CH_4 for the films were obtained by the integral barometric method on a thermostatically controlled installation with an MKS Baratron pressure sensor and an air thermostat. LabVIEW-based software was used to control the experiment. The experiments were carried out at 35 °C (in the case of comparison with the differential method data, at 50 °C) and upstream pressure in the range of 1–3 bar. Downstream pressure was maintained at ~10^{-6} bar; therefore, under the experimental conditions, the reverse diffusion of the penetrant was neglected. The permeability coefficients *P* were determined from the linear section of the gas pressure accumulation curve when the gas is passing through the polymer film into the calibrated volume (by the slope tangent of the linear dependence of the flow through the film when a steady-state mode is reached):

$$P = \frac{Vl}{St\Delta p} = \frac{\Delta p}{\Delta t}\frac{V_k T_0/(T_0+T)}{p_{atm}}\frac{l}{S(p_f - p_p)}, \quad (3)$$

where *l* is the thickness of the film under study, $\Delta p/\Delta t$ is the slope tangent of the integral curve, *S* is the working area of the membrane, V_k is the calibrated volume.

From the resulting data on the permeability coefficients, the values of the ideal selectivity α for different pairs of gases *i* and *j* were calculated:

$$\alpha = P_i/P_j. \quad (4)$$

The diffusion coefficients D were calculated by the Daynes–Barrer method using the time-lag θ:

$$D = l^2/6\theta, \quad (5)$$

where l is the thickness of the film.

The solubility coefficients S were calculated from the P and D experimental values according to the following formula

$$S = P/D. \quad (6)$$

The experimental errors were 5% and 10% for P and D, respectively; the calculation errors were 15% and 10% for S and α, respectively.

The densities of the resulting polymer films (ρ) were determined at room temperature (24 ± 2 °C) by hydrostatic weighing in isopropanol. The fractional free volume FFV was calculated using the Bondi method: $FFV = 1 - 1.3\ V_w/V_{sp}$, where V_w is the van der Waals volume of the monomer unit calculated by the Askadskii method [25], $V_{sp} = M/p$ is the specific occupied volume of the polymer, M is the molecular weight of the repeating unit of the polymer.

Synthesis

The synthesis and investigation of the structures and physicochemical properties of PBI-O-PhT-P and PBI-4MeO-6F were described in detail elsewhere [16, 17].

Conclusions

The gas transport characteristics of two new PBIs with bulky substituents and a hexafluoroisopropylidene group were studied at 35 °C. It was shown that, in terms of permeability, both of these polymers are at the level of previously studied PBIs with similar substituents. There is obvious evidence that the transport of CO_2 in phosphonethylated PBIs is accomplished through the mechanism of specific interactions, which is not observed in the PBI with fluorinated groups. Taking into account an increase in the selectivity of H_2/CO_2 with temperature, there is every reason to assume that the PBIs explored are promising for high-temperature gas separation processes.

Acknowledgements

This work was supported by the Russian Science Foundation (project no. 23-19-00222).

Access to electronic scientific resources was provided by INEOS RAS with support from the Ministry of Science and Higher Education of the Russian Federation.

Corresponding author

* E-mail: nru@ips.ac.ru (R. Yu. Nikiforov).

References

1. High Temperature Polymer Electrolyte Membrane Fuel Cells: Approaches, Status, and Perspectives, Q. Li, D. Aili, H. A. Hjuler, J. O. Jensen (Eds.), Springer, Cham, **2016**. DOI: 10.1007/978-3-319-17082-4
2. K. Y. Wang, M. Weber, T.-S. Chung, *J. Mater. Chem. A*, **2022**, *10*, 8687–8718. DOI: 10.1039/D2TA00422D
3. T. C. Merkel, M. Zhou, R. W. Baker, *J. Membr. Sci.*, **2012**, *389*, 441–450. DOI: 10.1016/j.memsci.2011.11.012
4. A. Yu. Alentiev, V. E. Ryzhikh, D. A. Syrtsova, N. A. Belov, *Russ. Chem. Rev.*, **2023**, *92*, RCR5083. DOI: 10.59761/RCR5083
5. A. Yu. Alentiev, V. E. Ryzhikh, N. A. Belov, *Polym. Sci., Ser. C*, **2021**, *63*, 181–198. DOI: 10.1134/S1811238221020016
6. H. B. Park, Y. M. Lee, in: Advanced Membrane Technology and Applications, N. N. Li, A. G. Fane, W. S. W. Ho, T. Matsuura (Eds.), Wiley, Hoboken, **2008**, ch. 24, pp. 633–669. DOI: 10.1002/9780470276280.ch24
7. J. H. Bitter, A. A. Tashvigh, *Ind. Eng. Chem. Res.*, **2022**, *61*, 6125–6134. DOI: 10.1021/acs.iecr.2c00645
8. M. Rezakazemi, M. Sadrzadeh, T. Matsuura, *Prog. Energy Combust. Sci.*, **2018**, *66*, 1–41. DOI: 10.1016/j.pecs.2017.11.002
9. D. R. Pesiri, B. Jorgensen, R. C. Dye, *J. Membr. Sci.*, **2003**, *218*, 11–18. DOI: 10.1016/s0376-7388(03)00129-7
10. S. C. Kumbharkar, P. B. Karadkar, U. K. Kharul, *J. Membr. Sci.*, **2006**, *286*, 161–169. DOI: 10.1016/j.memsci.2006.09.030
11. N. P. Panapitiya, S. N. Wijenayake, D. D. Nguyen, Y. Huang, I. H. Musselman, K. J. Balkus, J. P. Ferraris, *ACS Appl. Mater. Interfaces*, **2015**, *7*, 18618–18627. DOI: 10.1021/acsami.5b04747
12. L. Zhu, M. T. Swihart, H. Lin, *J. Mater. Chem. A*, **2017**, *5*, 19914–19923. DOI: 10.1039/C7TA03874G
13. K. A. Stevens, J. D. Moon, H. Borjigin, R. Liu, R. M. Joseph, J. S. Riffle, B. D. Freeman, *J. Membr. Sci.*, **2020**, *593*, 117427. DOI: 10.1016/j.memsci.2019.117427
14. X. Li, R. P. Singh, K. W. Dudeck, K. A. Berchtold, B. C. Benicewicz, *J. Membr. Sci.*, **2014**, *461*, 59–68. DOI: 10.1016/j.memsci.2014.03.008
15. Y. Jiao, M. Liu, Q. Wu, P. Zheng, W. Xu, B. Ye, H. Zhang, R. Guo, S. Luo, *J. Membr. Sci.*, **2023**, *672*, 121474. DOI: 10.1016/j.memsci.2023.121474
16. Iv. I. Ponomarev, I. I. Ponomarev, P. V. Petrovskii, Yu. A. Volkova, D. Yu. Razorenov, I. B. Goryunova, Z. A. Starikova, A. I. Fomenkov, A. R. Khokhlov, *Dokl. Chem.*, **2010**, *432*, 168–174. DOI: 10.1134/S0012500810060042
17. I. I. Ponomarev, Y. A. Volkova, K. M. Skupov, E. S. Vtyurina, I. I. Ponomarev, M. M. Ilyin, R. Y. Nikiforov, A. Y. Alentiev, O. M. Zhigalina, D. N. Khmelenin, T. V. Strelkova, A. D. Modestov, *Int. J. Mol. Sci.*, **2024**, *25*, 6001. DOI: 10.3390/ijms25116001
18. A. Yu. Alent'ev, V. E. Ryzhikh, N. A. Belov, *Polym. Sci., Ser. C*, **2020**, *62*, 238–258. DOI: 10.1134/S1811238220020010
19. V. V. Teplyakov, C. G. Durgar'yan, *Vysokomol. Soedin., Ser. A*, **1984**, *26*, 2159.
20. V. Teplyakov, P. Meares, *Gas Sep. Purif.*, **1990**, *4*, 66–74. DOI: 10.1016/0950-4214(90)80030-O
21. A. Yu. Alentiev, R. Yu. Nikiforov, I. S. Levin, D. A. Tsarev, V. E. Ryzhikh, D. A. Syrtsova, N. A. Belov, *Membr. Membr. Technol.*, **2023**, *5*, 430–439. DOI: 10.1134/S2517751623060021
22. D. A. Alentiev, R. Yu. Nikiforov, M. A. Rudakova, D. P. Zarezin, M. A. Topchiy, A. F. Asachenko, A. Yu. Alentiev, B. D. Bolshchikov, N. A. Belov, E. Sh. Finkelshtein, M. V. Bermeshev, *J. Membr. Sci.*, **2022**, *648*, 120340. DOI: 10.1016/j.memsci.2022.120340
23. E. M. Erdni-Goryaev, A. Yu. Alentiev, G. N. Bondarenko, A. B. Yaroslavtsev, E. Yu. Safronova, Yu. P. Yampolskii, *Pet. Chem.*, **2015**, *55*, 693–702. DOI: 10.1134/S0965544115090029
24. A. Y. Alentiev, D. A. Syrtsova, R. Yu. Nikiforov, V. E. Ryzhikh, N. A. Belov, K. M. Skupov, Yu. A. Volkova, I. I. Ponomarev, *Polymer*, **2024**, *308*, 127394. DOI: 10.1016/j.polymer.2024.127394
25. A. A. Askadskii, V. I. Kondrashchenko, Computer Materials Science, Nauchnyi Mir, Moscow, **1999**, vol. 1 (in Russian).